Available online at www.eccomasproceedia.org
Eccomas Proceedia SMART (2023) 829-839

ECCOMAS
Proceedia

X ECCOMAS Thematic Conference on Smart Structures and Materials
SMART 2023
D.A. Saravanos, A. Benjeddou, N. Chrysochoidis and T. Theodosiou (Eds)

PCA-BASED ACCELEROMETER DATA TRANSFORMATION IN OFFSHORE JACKET-TYPE WIND TURBINE SUPPORT STRUCTURES FOR INCIPIENT DAMAGE DETECTION

Y. Vidal[*,†], **R. Valdez**[‡], **and C. Tutivén**[‡,#]

[*] Control, Data, and Artificial Intelligence, CoDAlab
Department of Mathematics, Escola d'Enginyeria de Barcelona Est, EEBE
Universitat Politècnica de Catalunya, UPC
Campus Diagonal-Besós (CDB) 08019, Barcelona, Spain
e-mail: yolanda.vidal@upc.edu,
Web page: https://www.upc.edu/es

[†] Institut de Matemàtiques de la UPC - BarcelonaTech, IMTech
Pau Gargallo 14, 08028 Barcelona, Spain
Phone number: +34 934 137 309 Web page: https://imtech.upc.edu/en

[‡] Mechatronics Engineering
Faculty of Mechanical Engineering and Production Science, FIMCP
Escuela Superior Politécnica del Litoral, ESPOL
Campus Gustavo Galindo Km. 30.5 Vía Perimetral, P.O. Box 09-01-5863, Guayaquil, Ecuador
Phone number: +593 9 9103 5259,
e-mail: {rhakvald, cjtutive}@espol.edu.ec,
web page: https://www.espol.edu.ec

[#] Universidad ECOTEC, Km. 13.5 Samborondón, Samborondón, EC092303, Ecuador
Phone number: +593 04 3723400,
Web page: https://ecotec.edu.ec

Key words: Offshore wind turbine, structural health monitoring, damage detection, Principal Components Analysis, Mahalanobis Distance

Abstract. Global power capacity is increasingly being comprised by renewable energy sources, where wind farms stand out as paramount power stations. Therefore, the structural health of wind turbines (WTs) represents an essential factor in the energy industry. Specifically, offshore jacket-type WT supports are under critical operational and environmental conditions. Hence, a damage detection strategy is stated, considering several types of structural states and limitations in the quantity of acquired data. The proposed methodology consists of a PCA-based data transformation, in which initially known healthy data are used to be compared with a set of data to be diagnosed; then the damage or healthy states are predicted based on the Mahalanobis distance and threshold value. Because it is a semi-supervised technique, there is no requirement to have damage data on hand to construct the model. The strategy is tested in a scaled-down WT experimental tower.

Peer-review under responsibility of the organizing committee of SMART 2023.
doi: 10.7712/150123.9836.441277

1 INTRODUCTION

The consumption of coal and gas was expected to increase in 2022 due to the crisis facing the world today as a result of the conflict between Russia and Ukraine. However, this was not the case, at least not in the electrical industry. In reality, renewable energy sources completely met the increase in global electricity demand in the first half of 2022, halting the use of fossil fuels [1]. According to historical trends, the first half of 2022 saw a 3% increase in global power consumption over the same time in the previous year. Wind and solar met 77% of the total energy demand, while the rest was covered by hydro [1].

Wind energy production grew by a record 273 TWh in 2021 (up 17%) [2]. This growth rate was the highest among all renewable energy technologies and was 55% higher than what was achieved in 2020. However, to meet the requirements of the Net Zero Emissions by 2050 Scenario, which calls for nearly 7900 TWh of wind power generation in 2030, average annual capacity additions must be increased to almost 250 GW -more than twice the record growth of 2020- [2].

Offshore WTs, although not currently the most widely implemented, are experiencing growth. Offshore technology contributed around 22% of the 94 GW increase in overall wind capacity in 2021 [2]. A slowdown in global onshore growth combined with record additions of offshore capacity in China, which accounted for 80% of offshore growth, led to such a high percentage [2]. The expansion of onshore wind capacity is expected to continue at a steady rate in the upcoming years, while offshore systems are expected to expand much more quickly in both their current markets, the European Union and China, and new markets, the United States, Taipei and Japan. The energy generated by offshore turbines is of particular interest because it offers some advantages over onshore wind energy, including significant energy reserves, faster and steadier wind speeds, and less environmental impact [3]. However, offshore WTs are exposed to critical environmental conditions. One of the most affected components is the base structure, which is constantly affected by waves, scour, or currents [4]. Hence, each of them contributes to the uncertainty of the structural state and increases the probability of damage. The wind industry employs preventive maintenance techniques (planned maintenance) and corrective maintenance techniques (remedy failures) to minimize downtime caused by unforeseen damages. However, research must advance to the development of approaches based on the state of assets to achieve higher efficiency and lower maintenance costs (predictive maintenance) [5]. Therefore, for offshore WT structures, the development of a structural health monitoring (SHM) plan is essential.

Real-time sensing, identification, and evaluation of the safety and performance development of structures are all topics covered by SHM. An SHM system typically includes a number of sensors, data collecting devices, data transmission systems, databases for data management, data analysis and modeling, condition assessment and performance prediction, alarm devices, graphical user interfaces, software, and operating systems [6]. In the disciplines of mechanical, civil, and aeronautical engineering, SHM systems have been widely used. In the field of wind energy, having accurate predictions of the structural state of the wind turbine (WT) allows reducing operating and maintenance costs and extending the useful life of the structure [7]. Several SHM methodologies have been developed since damage detection is a critical functionality to improve the performance of WTs and its successful implementation depends on sensing technology and accurate data analysis [8]. For example, in [9] it is described how damage could be detected and supervised in grouted WT offshore connections due to the duration and number of acoustic emissions during bending tests, in which the acquired signals were correlated with load-displacement measurements. Furthermore, ultrasonic guided waves had been implemented to locate, classify and determine the severity of inner structural damage in offshore WT blades [10]. However, vibration-based methodologies have been preferred recently, as they are the most efficient in the early detection of failures

[11]. In [12], an SHM approach for offshore foundations is developed based on the variability of its resonance frequencies related to potential structural changes and the implementation of a nonlinear regression model that compensates for environmental variations. Furthermore, Oliveira et al. [13] define a similar methodology in which the modal properties of important WT modes are identified, which allows for damage detection at an initial stage in the WT support structure and continuous analysis of the dynamic properties of the turbine. In [14], a jacket-like support structure diagnostic methodology is proposed based on accelerometer-only measurements of vibration response and on two cascaded convolutional neural networks. Wang et al. [15] propose a variable selection algorithm based on multivariate principal component analysis (PCA), cost functions to maximize data variability, and two fault detection strategies based on the Hotelling T-squared statistic and the coefficients of the principal components. A foundation damage diagnosis methodology is described in [16], which uses vibration response accelerometer signals and, with a supervised approach, classifies the data with two different machine-learning algorithms, k nearest neighbor (k-NN) and quadratic-kernel support vector machine (SVM). Finally, Feijóo et al. [17] developed a damage detection strategy based on an autoencoder neural network that is unsupervised.

This work contributes to a vibration-based methodology in which the experimental acceleration response data from a scaled-down jacked-type WT laboratory tower are inspected to detect possible bolt loosening in a specific level of the jacket-type WT. First, the excitation of the wind, simulated as Gaussian white noise, is established as the only input signal. Then, data acquisition is performed by several accelerometers, and each data set obtained is re-shaped to handle data scarcity. The reshaped data set is then classified into a category depending on its future use and the conditions of the experiment. After that, column scaling and PCA are implemented for dimensionality reduction to obtain a healthy model of the WT. Finally, Mahalanobis distances are calculated for every test data sequence with respect to the healthy model, and a threshold value is then determined to analyze whether the aforementioned distance corresponds to a healthy WT or not. The proposed methodology offers a computationally inexpensive procedure, since testing a data set requires less than a minute, considering that the healthy model is already built. Furthermore, when only initial structural damage is taken into account, the results obtained are equally robust compared to other complex methodologies.

The structure of this work is as follows. Section 2 describes the setup of the WT laboratory tower where the data is acquired. Section 3 details the PCA-based damage detection methodology. The results are presented in Section 4. Finally, the conclusions are stated in Section 5.

2 EXPERIMENT SETUP

A scaled WT structure (as can be seen in Figure 1) is used for the current study. This model is 2.7 meters tall and is made up of a jacket base, a tower, and a nacelle. The methodology presented in this work is based only on acceleration measurements, for which eight triaxial acceleration sensors are installed at different positions of the turbine. Each of these sensors collects three signals (x-axis, y-axis, and z-axis accelerations), for which there are 24 acceleration measurements in total. Additionally, as is well known, depending on the wind speed WTs can operate in one of three distinct operating zones. For that reason, a shaker is used to induce vibration into the structure modifying the white noise (WN) signal amplitude (i.e., scaling the amplitude by 0.5, 1, and 2) simulating different wind speeds. In this work, only the region of operation where the winds are higher is considered, since it is where the turbine is more susceptible to possible damages (WN amplitude equal to 2). For more information about the experiment setup, see [18].

On the other hand, four distinct structural states are studied in relation to one of the bars of the WT jacket structure. The simulated states in experiments consist of loosening one metal bolt in the base, which joins a link to the central part of the structure in a specific level. In order to establish an exact pressure

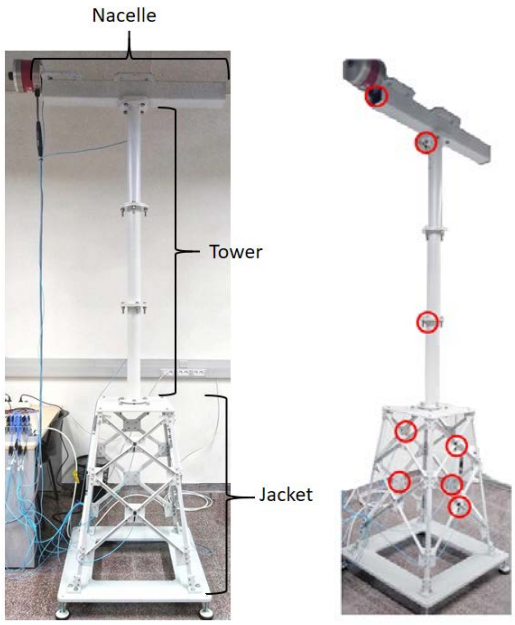

Figure 1: Scale structure with vibration sensors.

level to the bolt, a torquemeter is used. The healthy scenario for the structure consisted of having all the bolts at 12 Nm. Additionally, different damage scenarios are specified by setting the pressure on the bolts at 9 Nm and 6 Nm (to represent continuous bolt loosening) and removing them from the structure, representing total damage. In Figure 2 it is indicated the bolt where the modifications are performed to induce the different levels of damage. Additionally, in Figure 3 it is portrayed the scenario where the bolt is absent.

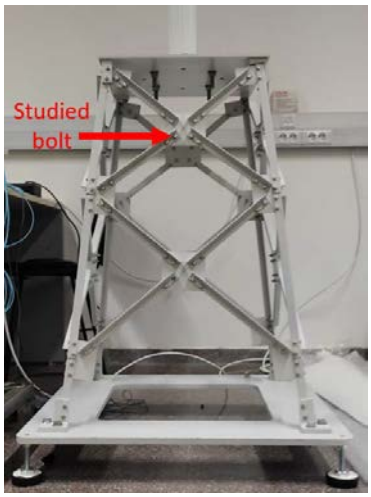

Figure 2: Location of the bolt where different damages are produced.

Figure 3: Damage type where the bolt is absent from the structure.

3 METHODOLOGY

The proposed technique, explained in this section, is based on the initial hypothesis. Data acquisition, data splitting, data reshaping, and, lastly, the development of a PCA data transformation strategy make up this process. The following is a description of each of those phases.

3.1 Data acquisition

The duration of each experimental test to acquire data is 60 seconds, with a sampling frequency of around 1.6 kHz. As a consequence, each of the 24 sensors obtains 99,097 timestamps. Below is a description of the trials carried out:

- Twenty healthy experimental tests (correctly tightened bolts at 12Nm).
- Twelve tests with bolt loosening fixed at 9 Nm.
- Twelve tests with bolt loosening fixed at 6 Nm.
- Twelve tests without a bolt.

The matrix $\mathbf{X}$ in equation (1) is presented as the general form of the measured data for one experimental case (the same representation is for all the experiments). The two sub-indices i and j are related to time instant (row) and the sensor (column), respectively. More precisely,

- $i = 1,\ldots,I$ identifies the time stamp, while I is the number of time stamps per experiment, equal to 99,097;
- $j = 1,\ldots,J$ represents the measuring sensor, while J is the total number of sensors, equal to 24.

$$\mathbf{X} = \begin{bmatrix} x_{1,1} & x_{1,2} & \cdots & x_{1,J} \\ x_{2,1} & x_{2,2} & \cdots & x_{2,J} \\ \vdots & \vdots & \ddots & \vdots \\ x_{I,1} & x_{I,2} & \cdots & x_{I,J} \end{bmatrix} \tag{1}$$

.

3.2 Data reshape

Since only a few minutes of data per experimental case is available for analysis and the quantity of features is limited by the number of sensors, a reshape of the original matrix is required for extracting more features from the data. Therefore, the matrix $\mathbf{X}$, described in (1), is modified into a new matrix $\mathbf{Y}$, where the information remains, but the shape of the resultant matrix is different in both dimensions. The matrix $\mathbf{Y}$ is obtained with the following steps (the reshaping process is done per experimental case):

1. A column of matrix $\mathbf{X}$ is transformed to a row vector of length 99,097;
2. The row vector is divided into M sequences of length O, each with unique data, where some final observations may have been omitted because they do not complete a sequence of length O;
3. The data sequences are arranged as rows, appending each of them beneath the last one;
4. Previous steps are repeated for all columns, generating new submatrices and appending them at the right of the last column in matrix $\mathbf{Y}$. The total horizontal sub-matrices in $\mathbf{Y}$ is 24.

For the above-mentioned procedure, a sequence's length O is calculated considering that unused observations should be minimized, resulting in a O value equal to 1,139. As a consequence, the number of data sequences M arranged in each submatrix is 87. Therefore, the matrix $\mathbf{Y}$ is detailed in Equation (2):

$$\mathbf{Y} = \left[\begin{array}{ccc|ccc|c|ccc} x_{1,1} & \cdots & x_{O,1} & x_{1,2} & \cdots & x_{O,2} & \cdots & x_{1,J} & \cdots & x_{O,J} \\ x_{O+1,1} & \cdots & x_{2\cdot O,1} & x_{O+1,2} & \cdots & x_{2\cdot O,2} & \cdots & x_{O+1,J} & \cdots & x_{2\cdot O,J} \\ \vdots & \ddots & \vdots & \vdots & \ddots & \vdots & \ddots & \vdots & \ddots & \vdots \\ x_{(M-1)\cdot O+1,1} & \cdots & x_{M\cdot O,1} & x_{(M-1)\cdot O+1,2} & \cdots & x_{M\cdot O,2} & \cdots & x_{(M-1)\cdot O+1,J} & \cdots & x_{M\cdot O,J} \end{array}\right], \quad (2)$$

where J is the total number of sensors; O represents the length of the data sequences; and $m = 1,\ldots,M$ identifies the sequence number, while M is the total number of sequences per experiment.

3.3 Data split

Data from the experiments are divided into different categories depending on their use in the next stage of the process: baseline construction, model validation (make predictions), or threshold calculation. Therefore, the relevance of splitting information relies on two of the main features of the novel methodology:

- To generate a model every time a new prediction is performed to detect damage, using the new data and a baseline dataset that consists of healthy data only;
- To compute a threshold with data from the new test and a separate set of healthy data, which allows discerning whether the new test is associated with a damage condition in the structure or not.

As a result, the healthy data is used to generate the reference model (constructed each time a prediction needs to be done), to determine the detection threshold, and to validate the operation of the proposed strategy when healthy data is the input to the model. On the other hand, all damage experiments are only used to verify if the methodology is capable of detecting damage when the input to the model is data related to damage. The data division is summarized as follows:

- Six healthy datasets to determine the baseline, for each white noise;
- Two healthy datasets to determine thresholds, for each white noise;
- Twelve healthy datasets to validate the model, for each white noise;
- All the datasets with damage to validate the model;

3.4 PCA data transformation for damage detection

For the proposed damage detection methodology, the Mahalanobis distance metric [19], and Principal Component Analysis (PCA) are implemented through several steps in which the original data is transformed into conclusive information about whether the WT support structure has been damaged or not.

Furthermore, four new matrices are established with the previously reshaped data matrices of each experiment. Two testing matrices ($\mathbf{T_1}$ and $\mathbf{T_2}$) are modeled with six different experiments each (could be healthy or with any type of damage). For both $\mathbf{T_1}$ and $\mathbf{T_2}$, each of the six reshaped matrices of the tests is appended one beneath the other in the corresponding testing matrix; Baseline and threshold matrices, $\mathbf{B}$ and $\mathbf{H}$ respectively, are obtained with healthy experiments. The baseline uses six experiments, while the threshold only uses two. To model $\mathbf{B}$ and $\mathbf{H}$, the reshaped matrices are processed with the same appending procedure as the testing matrices.

In PCA, the principal components are new variables obtained by a linear transformation of the original variables in the dataset. Furthermore, each component ensures that it is described in the directions (represented by eigenvectors) where the largest possible variance is, as well as orthogonal with respect to the other components, as detailed in [20]. During the determination of the principal components, a matrix $\mathbf{P}$ is obtained with the coefficients for a linear transformation in which other data is projected on the principal components. Both the matrix $\mathbf{P}$ and the principal components are implemented in the unsupervised methodology described afterwards.

1. The matrix $\mathbf{T_1}$ is adjoined under matrix $\mathbf{B}$. The resultant matrix $\mathbf{M}$ has 27,336 features or columns, as a result of the previous reshaping of all test data matrices. The new matrix undergoes column standardization before applying PCA, where the first 19 principal components are obtained. Therefore, each row of the new matrix $\hat{\mathbf{M}}$ has 19 columns and describes the original data projected in the principal components, having the same number of observations as $\mathbf{M}$. As a result of PCA, the projection matrix $\mathbf{P}$ is obtained for further linear transformation of data considering the same 19 principal components.

2. The matrices $\mathbf{T_2}$ and $\mathbf{H}$ are multiplied by the projection matrix $\mathbf{P}$, where the new matrices $\hat{\mathbf{T}}_\mathbf{2}$ and $\hat{\mathbf{H}}$ have their rows or observations represented in the 19 principal components.

3. The upper middle of the matrix $\hat{\mathbf{M}}$, which corresponds to the data of the baseline matrix $\mathbf{B}$ after PCA was applied, is split into a new matrix $\hat{\mathbf{B}}$ for further steps. This matrix provides information on the healthy condition of the support structure described in the principal components.

4. A list of Mahalanobis distances is determined considering each row of the threshold matrix $\hat{\mathbf{H}}$ and calculating the metric mentioned above with respect to the entire baseline matrix $\hat{\mathbf{B}}$. To determine the threshold value, the mean and standard deviation of the values in the list are considered. Therefore, the final threshold value is computed as the mean added three times the standard deviation. Assuming that the distances are normally distributed, three standard deviations from the

mean will give a 99.7% confidence that the distances calculated with healthy data will be equal to or below the threshold value. Therefore, damage cases will have Mahalanobis distances above the threshold.

5. For every row in matrix $\hat{\mathbf{T}}_\mathbf{2}$, a Mahalanobis distance is calculated with respect to the data in matrix $\hat{\mathbf{B}}$. This value is compared to the threshold: if it is greater, then damage has been detected in the structure.

The selected number of 19 principal components was determined based on an iterative process in which the proposed methodology was implemented, modifying only the number of components considered for PCA. Depending on whether there were too many components or not, the results were seriously affected on several experiments with specific conditions. Therefore, an optimum interval for the components was found: from 15 to 20. On the other hand, the column standardization prior to PCA is performed subtracting the column's mean to the old value and dividing the result to the column's standard deviation, as stated below.

$$x_{new} = \frac{x - \mu_{column}}{\sigma_{column}}$$

In Figure 4 it is portrayed how the several data sets used in the methodology are modified through the steps aforementioned.

4 RESULTS

As described in the last step of the methodology, each row of the matrix $\hat{\mathbf{T}}_\mathbf{2}$ was evaluated to determine if its information indicated damage to the base structure or not. In Table 1 the percentages shown represent the proportion of accurate detections for all the analyzed experimental scenarios, considering the different structural states at the analyzed level of the support structure and with a scale factor of 2 for the amplitude WN.

The results described in Table 1 indicate that all the experimental cases explored have an accuracy above 99% in predicting their true structural state. Furthermore, each damage detection process is completed on an average time of 38.13 seconds. The results of table 1 are depicted with a confusion

Table 1: Correct detection percentages for each structural state.

Structural state	**2 WN**
12 Nm	99.43%
9 Nm	100.00%
6 Nm	100.00%
Without bolt	100.00%

matrix in table 2. An evaluated data sequence through the methodology is considered a testing unit. Hence, the values described in the following table represent the number of data sequences classified into the corresponding predicted and true structural state. Based on table 2, the false positives and negatives are significantly less compared to their corresponding true category.

Furthermore, the results of the confusion matrix are evaluated based on several performance metrics in the following table, obtaining percentages greater than 99%.

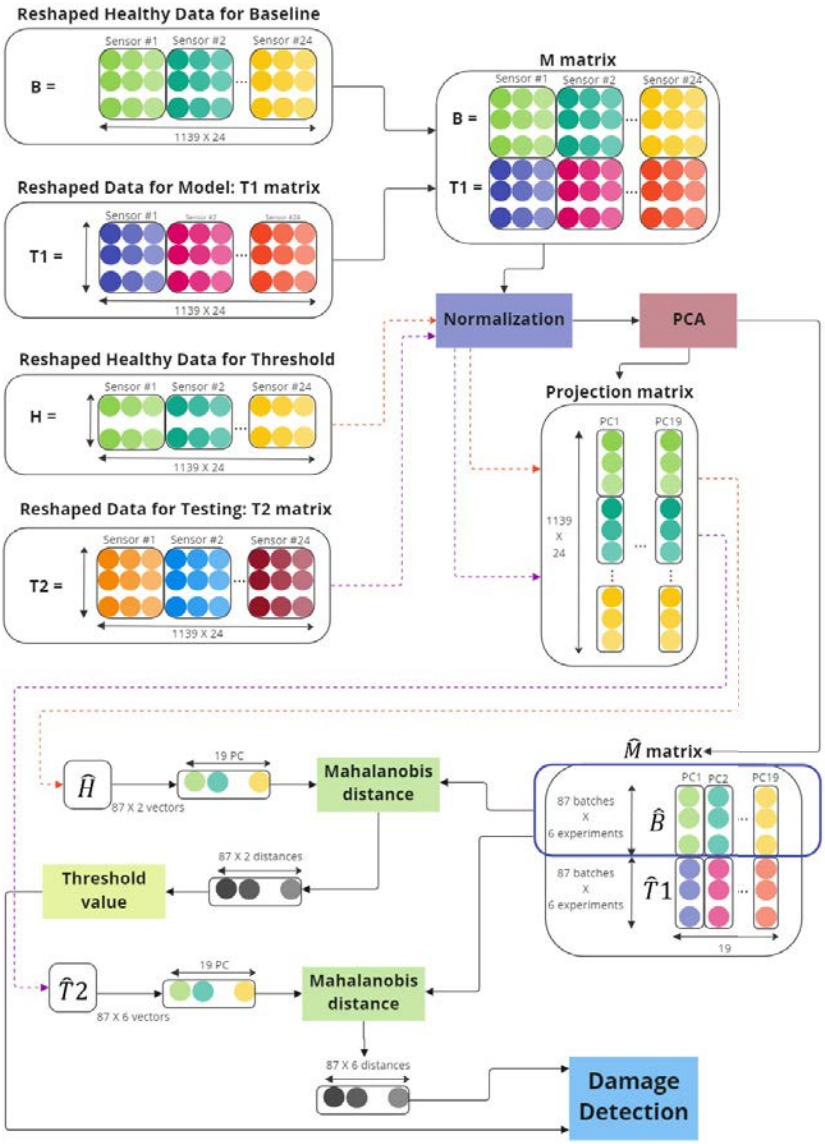

Figure 4: Methodology's flowchart.

Table 2: Confusion matrix for the testing data under the proposed damage detection methodology.

		Predicted structural state	
		Healthy	Damaged
True structural state	Healthy	504	18
	Damaged	0	1566

5 CONCLUSIONS

In this study, the stated structural health monitoring strategy was tested using an approach that is entirely based on the response to vibrations. The method was tested in a laboratory setting, where the

Table 3: Metrics of the confusion matrix considering all types of structural damage.

Sensitivity	0.966
Specificity	1.000
Precision	1.000
Accuracy	0.991
F1 Score	0.983

researchers investigated various levels of severity of structural damage when a metal bolt at the base that attaches a link to the center of the jacket structure at a specific level loosens.

The proposed methodology offers a computationally inexpensive procedure, with a mean detection time of 38.13 seconds. The data-augmented SHM methodology shows exceptional performance, with all metrics considered (sensitivity, specificity, precision, accuracy, and F1-score) yielding results greater than 96.6%. In particular, this PCA-based methodology obtained an accuracy of 99.1%, and only had 18 false positives and zero false negatives out of a total of 2088 total samples.

However, the main disadvantage, which will be faced as an immediate future work, is that it is necessary to validate the proposed strategy in a more realistic environment that takes into account various environmental and operational conditions. For example, one solution is to use a vibration test system based on a wave generating channel for offshore wind turbine jacket foundations of laboratory scale, such as the one proposed in [21].

6 ACKNOWLEDGEMENTS

This work is partially funded by the Spanish Agencia Estatal de Investigación (AEI) - Ministerio de Economía, Industria y Competitividad (MINECO), and the Fondo Europeo de Desarrollo Regional (FEDER) through the research project PID2021-122132OB-C21, and by the Generalitat de Catalunya through the research project 2021 SGR 01044.

REFERENCES

[1] D. Jones, Global electricity review 2022, Tech. rep., Ember (mar 2022).

[2] P. Bojek, Wind electricity: Tracking report - september 2022, Tech. rep., International Energy Agency (sep 2022).

[3] K. Wei, S. Arwade, A. Myers, Incremental wind-wave analysis of the structural capacity of offshore wind turbine support structures under extreme loading, Engineering Structures 79 (2014) 58.

[4] M. Arshad, B. O´Kelly, Offshore wind-turbine structures: a review, Energy 166 (4) (2013) 144–145.

[5] J. Daily, J. Peterson, Predictive maintenance: How big data analysis can improve maintenance, Supply Chain Integration Challenges in Commercial Aerospace: A Comprehensive Perspective on the Aviation Value Chain (2017) 267–278.

[6] Y. Bao, Z. Chen, S. Wei, Y. Xu, Z. Tang, H. Li, The state of the art of data science and engineering in structural health monitoring, Engineering 5 (2) (2019) 234–242.

[7] M. Martinez-Luengo, A. Kolios, L. Wang, Structural health monitoring of offshore wind turbines: A review through the statistical pattern recognition paradigm, Renewable and Sustainable Energy Reviews 64 (2016) 94.

[8] C. Chen, J.-R. Lee, H.-J. Bang, Structural health monitoring for a wind turbine system: a review of damage detection methods, Measurement Science and Technology 19 (2008) 3.

[9] N. Tziavos, H. Hemida, S. Dirar, M. Papaelias, N. Metje, Structural health monitoring of grouted connections for offshore wind turbines by means of acoustic emission: An experimental study, Renewable Energy 147 (2019) 130.

[10] Y. Du, S. Zhou, X. Jing, Y. Peng, H. Wu, N. Kwok, Damage detection techniques for wind turbine blades: A review, Mechanical Systems and Signal Processing (2019) 8.

[11] F. Santos, A. Teixeira, C. Guedes, Floating Offshore Wind Farms, Springer International Publishing, 2016, Ch. Operation and Maintenance of Floating Offshore Wind Turbines, p. 186.

[12] W. Weitjens, T. Verbelen, G. De Sitter, C. Devriendt, Foundation structural health monitoring of an offshore wind turbine—a full-scale case study, Structural Health Monitoring 15 (4) (2016) 1.

[13] G. Oliveira, F. Magalhães, A. Cunha, E. Caetano, Vibration-based damage detection in a wind turbine using 1 year of data, Structural Control and Health Monitoring 25 (11) (2018) 2.

[14] J. Baquerizo, C. Tutivén, B. Puruncajas, Y. Vidal, J. Sampietro, Siamese neural networks for damage detection and diagnosis of jacket-type offshore wind turbine platforms, Mathematics 10 (7) (2022) 1131.

[15] Y. Wang, X. Ma, P. Qian, Wind turbine fault detection and identification through pca-based optimal variable selection, IEEE Transactions on Sustainable Energy 9 (4) (2018) 1628.

[16] Y. Vidal, G. Aquino, F. Pozo, J. E. M. Gutiérrez-Arias, Structural health monitoring for jacket-type offshore wind turbines: Experimental proof of concept, Sensors 20 (7) (2020).

[17] M. d. C. Feijóo, Y. Zambrano, Y. Vidal, C. Tutivén, Unsupervised damage detection for offshore jacket wind turbine foundations based on an autoencoder neural network, Sensors 21 (10) (2021) 3333.

[18] B. Puruncajas, Y. Vidal, C. Tutivén, Vibration-response-only structural health monitoring for offshore wind turbine jacket foundations via convolutional neural networks, Sensors 20 (12) (2020) 3429.

[19] R. De Maesschalck, D. Jouan-Rimbaud, D. L. Massart, The mahalanobis distance, Chemometrics and Intelligent Laboratory Systems 50 (2000) 4.

[20] H. Abdi, L. Williams, Principal component analysis, Wiley Interdisciplinary Reviews: Computational Statistics 2 (4) (2010) 434.

[21] Á. Encalada-Dávila, L. Pardo, Y. Vidal, E. Terán, C. Tutivén, Conceptual design of a vibration test system based on a wave generator channel for lab-scale offshore wind turbine jacket foundations, Journal of Marine Science and Engineering 10 (9) (2022) 1247.